

Multi-Paradigm Collaborative Adversarial Attack Against Multi-Modal Large Language Models

Yuanbo Li¹, Tianyang Xu¹, Cong Hu¹, Tao Zhou¹, Xiao-Jun Wu^{1*}, Josef Kittler²

¹School of Artificial Intelligence and Computer Science, Jiangnan University, Wuxi, China

²Centre for Vision, Speech and Signal Processing (CVSSP), University of Surrey, Guildford, UK

liyuanbo12138@163.com, {tianyong_xu, conghu, 8202407042, wu_xiaojun}@jiangnan.edu.cn
j.kittler@surrey.ac.uk

Abstract

The rapid progress of Multi-Modal Large Language Models (MLLMs) has significantly advanced downstream applications. However, this progress also exposes serious transferable adversarial vulnerabilities. In general, existing adversarial attacks against MLLMs typically rely on surrogate models trained within a single learning paradigm and perform independent optimisation in their respective feature spaces. This straightforward setting naturally restricts the richness of feature representations, delivering limits on the search space and thus impeding the diversity of adversarial perturbations. To address this, we propose a novel Multi-Paradigm Collaborative Attack (MPCAttack) framework to boost the transferability of adversarial examples against MLLMs. In principle, MPCAttack aggregates semantic representations, from both visual images and language texts, to facilitate joint adversarial optimisation on the aggregated features through a Multi-Paradigm Collaborative Optimisation (MPCO) strategy. By performing contrastive matching on multi-paradigm features, MPCO adaptively balances the importance of different paradigm representations and guides the global perturbation optimisation, effectively alleviating the representation bias. Extensive experimental results on multiple benchmarks demonstrate the superiority of MPCAttack, indicating that our solution consistently outperforms state-of-the-art methods in both targeted and untargeted attacks on open-source MLLMs. The code is released at <https://github.com/LiYuanBoJNU/MPCAttack>.

1. Introduction

The rapid advancement of multi-modal large language models (MLLMs) [1, 2, 45, 52] has substantially enhanced the capability of artificial intelligence systems to achieve

*Corresponding Author

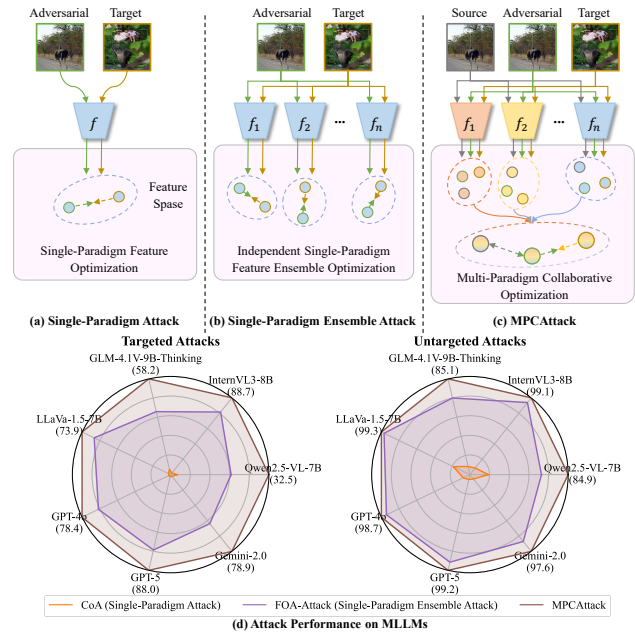


Figure 1. A comparison of the proposed MPCAttack with typical attack solutions. (a) and (b) show previous approaches based on a single learning paradigm (e.g., CoA [48], FOA-Attack [25]), while being limited by their transferability caused by restricted feature diversity and independent optimisation. (c) illustrates the core concept of MPCAttack, which integrates features from multiple learning paradigms and performs collaborative optimisation to enhance generalisation and transferability. Models and dashed ellipses in different colours represent the feature spaces of models delivered by different learning paradigms. (d) presents the attack success rates of different methods, where our MPCAttack obtains superior performance across various MLLMs consistently.

joint understanding and reasoning across visual and textual modalities. However, as MLLMs have received wide attention in safety-critical domains, growing concerns have emerged regarding their robustness and security. Recent

studies indicate that MLLMs, similar to unimodal vision or language models, are highly vulnerable to adversarial attacks [11, 26, 39, 49, 51]. By introducing well-designed perturbations into visual inputs, adversaries can manipulate the model’s perception and reasoning processes, leading to incorrect or misleading textual responses. These vulnerabilities expose fundamental weaknesses in multi-modal feature representations and highlight the pressing need for powerful adversarial attack frameworks to rigorously assess the security of MLLMs.

Existing studies have proposed various adversarial attack frameworks against MLLMs to investigate their vulnerabilities, with a major concern being raised against transferable adversarial attacks [5, 18, 23, 50]. Particularly, these attacks leverage adversarial examples generated from white-box surrogate models to mislead black-box target models. However, existing transferable attacks [25, 29, 48] against MLLMs typically rely on surrogate models trained under a single learning paradigm, such as cross-modal alignment (*e.g.*, CLIP [37]), to craft adversarial examples. Although these transferable attacks promote progress in the construction of transferable adversarial examples, two critical issues remain to be addressed. **(1) Single-paradigm representation constraint.** Optimising adversarial perturbations within a single learning paradigm confines to a limited feature space, thus leading to reduced diversity and poor generalisation. The underlying reason lies in the fact that each paradigm captures only part of the multi-modal semantics. For instance, the cross-modal alignment paradigm [37] focuses on modality matching, the multi-modal understanding paradigm [34] captures abstract semantic relations, and the visual self-supervised paradigm [34] emphasises low-level visual cues. As a result, perturbations generated from a single paradigm often overfit its own representational bias, which performs ineffective transferability across different MLLMs. **(2) Independent feature optimisation without collaboration.** Existing attempts typically treat features from different surrogate models as independent optimisation objectives, with simple fusion strategies being used for final aggregation. This independent optimisation strategy overlooks the potential semantic complementarity between different representation spaces, thereby constraining the optimisation process within each local feature space, thus limiting its ability to capture global semantic relationships. The lack of coordination among features can lead to redundant gradient directions, causing the perturbation optimisation to fall into local optima and consequently weakening the transferability of the generated adversarial examples.

Drawing on this, we propose a novel Multi-Paradigm Collaborative Adversarial Attack framework (MPCAttack) that enhances the transferability of adversarial examples across MLLMs. MPCAttack fully integrates multiple large-scale learning paradigms, such as cross-modal

alignment, multi-modal understanding, and visual self-supervised learning, to construct more comprehensive visual and semantic feature representations. Through a Multi-Paradigm Collaborative Optimisation (MPCO) strategy, MPCAttack performs contrastive matching optimisation on aggregated features and adaptively emphasises the most informative regions within each paradigm. This collaborative mechanism effectively alleviates the representation bias and local optimum problems caused by single paradigm optimisation, thereby improving the global generalisation ability of adversarial perturbations. As shown in Figure 1, MPCAttack enhances the global expressiveness of perturbations through coordinated optimisation of multi-paradigm features, achieving stronger adversarial transferability across heterogeneous MLLM architectures. Extensive experiments on multiple benchmark datasets demonstrate that MPCAttack significantly outperforms state-of-the-art (SOTA) methods in both targeted and untargeted attack scenarios against open source and closed source MLLMs, confirming its effectiveness and universality. We summarise the main contributions as follows:

- MPCAttack, a novel adversarial attack framework that supports both targeted and non-targeted attacks, effectively generating transferable adversarial examples against MLLMs.
- A joint adversarial optimisation strategy, harmonising aggregated features derived from multiple large-scale learning paradigms through multi-paradigm collaborative optimisation.
- Extensive experimental analysis demonstrates that MPCAttack achieves superior attack performance compared to SOTA methods, highlighting the importance of multi-paradigm collaboration in revealing the vulnerabilities of MLLMs.

2. Related Work

2.1. Adversarial Attacks

Adversarial attacks are a key area for evaluating model robustness, exposing vulnerabilities in deep neural networks through carefully designed perturbations [10, 16, 27, 28, 32, 38]. With the rise of multimodal models processing both visual and textual inputs, multimodal adversarial attacks have gained increasing attention, particularly in black-box settings focused on improving transferability [5, 15, 18, 24]. AttackVLM [51] aligns image-text and image-image features using pretrained vision-language models to generate targeted attacks on MLLMs. AnyAttack [50] leverages self-supervised contrastive learning on large unlabeled datasets to produce targeted adversarial examples without labels. X-Transfer [23] dynamically selects a few suitable surrogate models from a large search space to create universally transferable examples. Chain of Attack (CoA) [48] iteratively

updates adversarial examples through multimodal semantic optimization, enhancing transferability and efficiency. M-Attack [29] applies image augmentations and CLIP ensemble surrogates for robust attacks on closed-source MLLMs like GPT-4o. FOA-Attack [25] further improves attack effectiveness using Feature Optimal Alignment and dynamic model weight integration.

2.2. Multi-Modal Large Language Models

Multi-modal large language models (MLLMs) achieve significant improvements in multi-modal understanding and reasoning by integrating visual and textual information. These models learn rich visual-semantic representations from large-scale image-text data, demonstrating excellent performance in tasks such as image captioning [6, 21, 43], visual question answering [33, 35], and cross-modal reasoning [20, 47]. Open-source MLLMs such as LLaVA [30, 31], Qwen-VL [2], and InternVL [7, 53] are jointly trained on large-scale image-text datasets, enabling them to generate high-quality multimodal textual responses while supporting complex visual understanding. Some closed-source commercial models, such as GPT-5, Claude, and Gemini [8, 42], further enhance multi-modal understanding in terms of complex reasoning and real-world adaptability. Despite their strong performance in multi-modal understanding, MLLMs still face significant challenges in adversarial robustness. This work exposes the security vulnerabilities of MLLMs against MPCAttack, providing new insights for improving their robustness.

2.3. Large-Scale Learning Paradigms

With the rapid growth of computational power and data scale, large-scale representation learning has achieved remarkable progress in visual and semantic understanding, giving rise to several dominant paradigms that underpin modern multimodal and vision-centric systems [13, 14, 17, 46]. In this study, we consider three representative paradigms: Cross-Modal Alignment [22, 41], Multi-modal Understanding [2, 31, 53], and Visual Self-Supervised Learning [3, 19, 40]. Cross-Modal Alignment, exemplified by vision-language models (VLMs) such as CLIP [37] and SigLIP [44], learns the correspondence between large-scale image and text pairs within a shared feature space, thereby achieving efficient feature alignment and significantly enhancing cross-modal representation consistency and generalization. Multi-modal Understanding, represented by MLLMs such as InternVL [53] and Qwen-VL [2], goes beyond feature alignment by integrating visual and textual representations within a unified joint space, enabling deep understanding and multi-step reasoning over visual information. Visual Self-Supervised Learning focuses on learning visual representations from large-scale unlabeled image data, as seen in models like DINOv2 [34], which provide

high-quality visual features for downstream multimodal tasks. These large-scale learning paradigms collectively provide complementary perspectives on visual semantics, encompassing aspects ranging from unimodal structural encoding to multimodal alignment and understanding, thereby forming the foundation of MPCAttack framework.

3. Methodology

3.1. Preliminaries

Given a source image x_s and a target image x_t , the goal of transferable adversarial attacks against MLLMs is to leverage the surrogate model f to generate an adversarial example $x_{adv} = x_s + \delta$, such that the output response of x_{adv} on the target MLLMs is as close as possible to the output response or ground-truth answer of x_t . Formally, a transferable adversarial attack can be formulated as an optimization problem that minimizes a feature distance or similarity loss on the surrogate model, subject to perceptual imperceptibility or norm constraints:

$$\min_{\delta} \mathcal{L}(f(x_s + \delta), f(x_t)), \quad \text{s.t. } \|\delta\|_{\infty} \leq \epsilon, \quad (1)$$

where \mathcal{L} represents the loss function and ϵ represents the maximum perturbation strength.

3.2. Multi-Paradigm Collaborative Attack

Most existing studies [25, 29] rely on surrogate models based on a single learning paradigm to generate adversarial examples. Although such methods can achieve certain attack effectiveness on models with similar architectures, they struggle to generalize across diverse representation spaces of target models due to significant differences in feature representations among different paradigms. Consequently, adversarial examples generated from the single-paradigm surrogates often exhibit limited transferability. To address this limitation, we propose a Multi-Paradigm Collaborative Adversarial Attack (MPCAttack) framework. The core idea is to fully exploit the visual and semantic features captured by different learning paradigms and perform feature-level collaborative optimization, thereby generating adversarial examples with enhanced generalization and transferability across MLLMs.

An overview of the proposed MPCAttack framework is illustrated in Figure 2. In the adversarial example generation stage, given a target image x_t and a source image x_s , we first randomly initialize an adversarial perturbation δ and apply it to x_s to obtain the adversarial example $x_{adv} = x_s + \delta$. Subsequently, MPCAttack simultaneously employs image encoders from three types of large-scale learning paradigms, including the cross-modal alignment paradigm f_{c_l} (e.g., CLIP), the multi-modal understanding paradigm f_m (e.g., InternVL3), and the visual self-supervised learning paradigm f_v (e.g., DINOv2), to extract

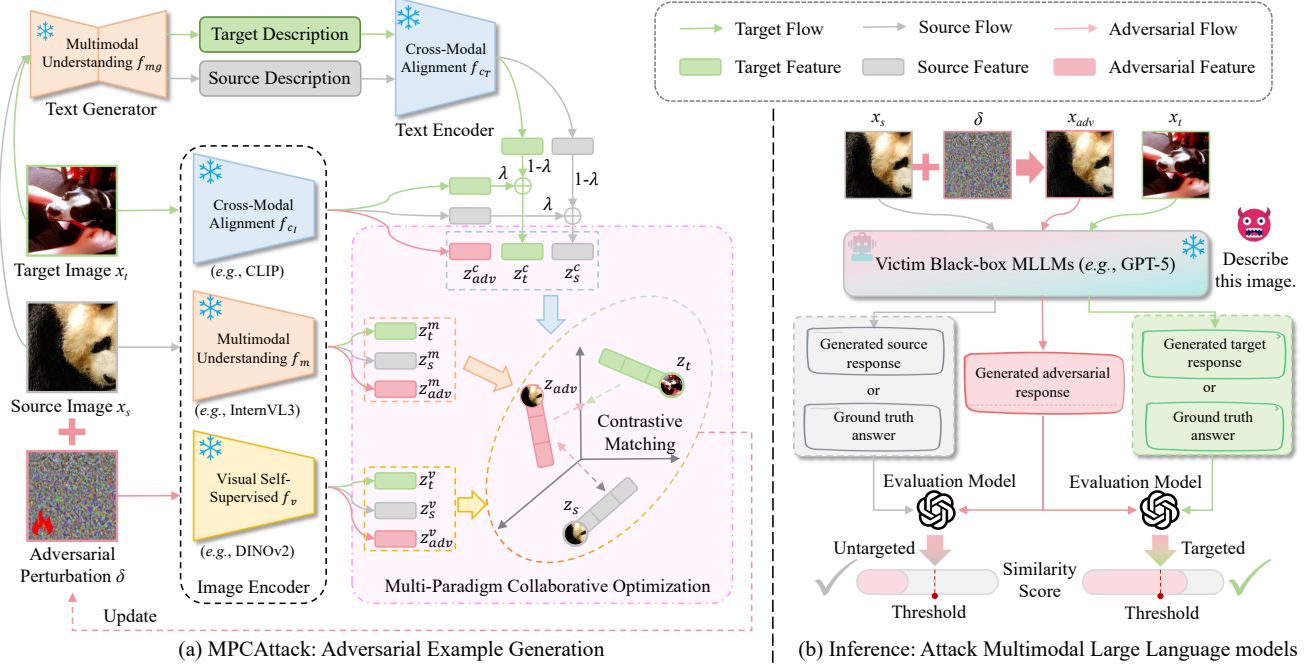


Figure 2. Overview of the proposed MPCAttack: (a) Pipeline for MPCAttack in adversarial examples generation. (b) Pipeline for attacking MLLMs.

image feature representations of x_t , x_s , and x_{adv} :

$$\begin{aligned} z_s^{cI}, z_t^{cI}, z_{adv}^{cI} &= f_{cI}(x_s), f_{cI}(x_t), f_{cI}(x_{adv}) \\ z_s^m, z_t^m, z_{adv}^m &= f_m(x_s), f_m(x_t), f_m(x_{adv}) \\ z_s^v, z_t^v, z_{adv}^v &= f_v(x_s), f_v(x_t), f_v(x_{adv}). \end{aligned} \quad (2)$$

The cross-modal alignment paradigm is typically trained on large-scale image–text pairs to optimize the consistency between visual and textual encoders within a shared semantic space, thereby learning high-quality aligned visual-textual embeddings. The multi-modal understanding paradigm jointly trains visual encoders with language models, enabling reasoning and generation across modalities within a unified semantic space. To fully exploit the complementary advantages of these two paradigms in semantic abstraction and representation, we input the x_t and x_s into the text generator of the multi-modal understanding model f_{mg} to extract the semantic information of x_t and x_s , generating the target description and source description, respectively. These generated descriptions are then encoded by the text encoder f_{cT} of the cross-modal alignment model to obtain high-level semantic feature representations:

$$z_s^{cT}, z_t^{cT} = f_{cT}(f_{mg}(x_s)), f_{cT}(f_{mg}(x_t)). \quad (3)$$

The image and text features extracted from the cross-modal alignment model are fused through weighted integration to yield joint feature representations that possess stronger se-

mantic consistency and cross-modal representation:

$$\begin{aligned} z_s^c &= \lambda \cdot z_s^{cI} + (1 - \lambda) \cdot z_s^{cT} \\ z_t^c &= \lambda \cdot z_t^{cI} + (1 - \lambda) \cdot z_t^{cT}, \end{aligned} \quad (4)$$

where λ is a weighting factor controlling the balance between visual and textual contributions.

Multi-Paradigm Collaborative Optimization. Different learning paradigms emphasize distinct aspects of feature representation within their respective embedding spaces. Optimizing adversarial perturbations directly within a single paradigm-specific space often causes the perturbation to overfit the representational bias of that paradigm, leading to suboptimal solutions and limited transferability. Therefore, we propose a Multi-Paradigm Collaborative Optimization (MPCO) strategy, which leverages feature representations from multiple learning paradigms to encourage adversarial perturbations to adaptively focus on the most informative regions across paradigms, thereby enhancing semantic generalization and transferability. Specifically, these multi-paradigm features are concatenated to form multi-paradigmatic feature representation:

$$\begin{aligned} z_s &= \left[\frac{z_s^c}{\|z_s^c\|_2}, \frac{z_s^m}{\|z_s^m\|_2}, \frac{z_s^v}{\|z_s^v\|_2} \right] \\ z_t &= \left[\frac{z_t^c}{\|z_t^c\|_2}, \frac{z_t^m}{\|z_t^m\|_2}, \frac{z_t^v}{\|z_t^v\|_2} \right] \\ z_{adv} &= \left[\frac{z_{adv}^c}{\|z_{adv}^c\|_2}, \frac{z_{adv}^m}{\|z_{adv}^m\|_2}, \frac{z_{adv}^v}{\|z_{adv}^v\|_2} \right]. \end{aligned} \quad (5)$$

Table 1. Performance of ASR (%) and AvgSim on open-source MLLMs across both targeted and untargeted settings on ImageNet dataset.

Targeted	Victim Black-box Open-Source Models									
	Qwen2.5-VL-7B		InternVL3-8B		LLaVa-1.5-7B		GLM-4.1V-9B-Thinking		Average	
	ASR(↑)	AvgSim(↑)	ASR(↑)	AvgSim(↑)	ASR(↑)	AvgSim(↑)	ASR(↑)	AvgSim(↑)	ASR(↑)	AvgSim(↑)
AnyAttack	0.8	0.0365	1.0	0.0323	1.2	0.0329	1.3	0.0381	1.08	0.0350
CoA	0.1	0.0232	0.2	0.0203	0.1	0.0158	0.3	0.0257	0.18	0.0213
M-Attack	17.3	0.1919	68.1	0.5361	59.9	0.4954	31.0	0.3118	44.08	0.3838
FOA-Attack	20.0	0.2222	72.3	0.5700	63.8	0.5162	38.3	0.3522	48.60	0.4152
MPCAttack	32.5	0.3191	88.7	0.6678	73.9	0.5905	58.2	0.4756	63.33	0.5133
Untargeted	Victim Black-box Open-Source Models									
	Qwen2.5-VL-7B		InternVL3-8B		LLaVa-1.5-7B		GLM-4.1V-9B-Thinking		Average	
	ASR(↑)	AvgSim(↓)	ASR(↑)	AvgSim(↓)	ASR(↑)	AvgSim(↓)	ASR(↑)	AvgSim(↓)	ASR(↑)	AvgSim(↓)
AnyAttack	37.8	0.5344	16.6	0.6875	28.2	0.6029	12.8	0.7240	23.85	0.6372
CoA	15.9	0.7040	8.5	0.7691	18.6	0.6869	7.2	0.7826	12.55	0.7357
X-Transfer	66.2	0.3178	56.8	0.3733	67.6	0.2919	33.3	0.5532	55.98	0.3841
M-Attack	54.3	0.3982	90.8	0.1417	94.9	0.0819	61.2	0.3696	75.30	0.2479
FOA-Attack	61.8	0.3589	93.0	0.1204	96.3	0.0659	68.1	0.3227	79.80	0.2170
MPCAttack	84.9	0.1919	99.1	0.0341	99.3	0.0186	85.1	0.1825	92.10	0.1068

Table 2. Performance of ASR (%) and AvgSim on closed-source MLLMs across both targeted and untargeted settings on ImageNet dataset.

Targeted	Victim Black-box Closed-Source Models									
	GPT-4o		GPT-5		Claude-3.5		Gemini-2.0		Average	
	ASR(↑)	AvgSim(↑)	ASR(↑)	AvgSim(↑)	ASR(↑)	AvgSim(↑)	ASR(↑)	AvgSim(↑)	ASR(↑)	AvgSim(↑)
AnyAttack	0.8	0.0315	0.8	0.0306	0.4	0.0272	0.4	0.0202	0.6	0.0274
CoA	0.1	0.0199	0.1	0.0205	0.1	0.0207	0.2	0.0159	0.125	0.0193
M-Attack	57.6	0.4804	67.6	0.5338	3.5	0.0970	49.2	0.4148	44.48	0.3815
FOA-Attack	63.9	0.5153	69.3	0.5580	7.3	0.1105	50.4	0.4504	47.73	0.4086
MPCAttack	78.4	0.5991	88.0	0.6502	8.2	0.1183	78.9	0.5991	63.38	0.4917
Untargeted	Victim Black-box Closed-Source Models									
	GPT-4o		GPT-5		Claude-3.5		Gemini-2.0		Average	
	ASR(↑)	AvgSim(↓)	ASR(↑)	AvgSim(↓)	ASR(↑)	AvgSim(↓)	ASR(↑)	AvgSim(↓)	ASR(↑)	AvgSim(↓)
AnyAttack	13.4	0.7182	7.6	0.7811	42.2	0.5002	12.2	0.7081	18.85	0.6769
CoA	7.4	0.7633	5.1	0.8079	36.1	0.5595	5.5	0.7964	13.53	0.7318
X-Transfer	55.4	0.4048	41.4	0.4956	55.7	0.4008	43.6	0.4677	49.03	0.4422
M-Attack	91.7	0.1413	88.7	0.1596	53.2	0.4265	81.3	0.2222	78.73	0.2374
FOA-Attack	93.0	0.1266	90.7	0.1420	61.8	0.3702	85.0	0.1898	82.63	0.2072
MPCAttack	98.7	0.0500	99.2	0.0524	66.7	0.3258	97.6	0.0613	90.55	0.1224

Here, each extracted feature is ℓ_2 -normalized to maintain scale consistency across paradigms. Then, MPCO performs contrastive matching on the aggregated features to achieve global-level collaborative optimization of adversarial representations. Specifically, the contrastive matching minimizes the distance between z_{adv} and z_t while maximizing the distance between z_{adv} and z_s , thereby guiding the perturbation direction toward global consistency under the joint representation of different paradigm features. The optimization objective can be formalized as follows:

$$\mathcal{L} = -\log \frac{\exp(\text{sim}(z_{adv}, z_t) / \omega \cdot \tau)}{\exp(\text{sim}(z_{adv}, z_t) / \tau) + \exp(\text{sim}(z_{adv}, z_s) / \tau)}, \quad (6)$$

where $\text{sim}(\cdot, \cdot)$ represents cosine similarity, τ is a temperature coefficient controlling the sharpness of similarity distribution, and ω is a balancing factor that regulates the trade-off between attracting positive pairs and repelling nega-

tive pairs. By aggregating features from multiple learning paradigms, MPCO expands the global receptive field and focuses optimization on the most discriminative semantic regions. This mitigates the representational bias of single-paradigm models, yielding richer, more consistent global representations and thereby enhancing the transferability of adversarial examples to unseen MLLMs.

During the inference phase attacking MLLMs, the generated adversarial examples are fed into the victim black-box MLLM (e.g., GPT-5) to obtain the adversarial response. Meanwhile, the source and target images are separately input into the same victim model to generate the source response and target response, respectively. Subsequently, all three responses are passed to an evaluation model (e.g., GPT-4o-mini). For untargeted attacks, the semantic similarity between the source response and the adversarial response is computed, whereas for targeted attacks, the sim-

Table 3. Performance of ASR (%) and AvgSim on open-source MLLMs across both targeted and untargeted settings on Flickr30K dataset.

Targeted	Victim Black-box Open-Source Models									
	Qwen2.5-VL-7B		InternVL3-8B		LLaVa-1.5-7B		GLM-4.1V-9B-Thinking		Average	
	ASR(↑)	AvgSim(↑)	ASR(↑)	AvgSim(↑)	ASR(↑)	AvgSim(↑)	ASR(↑)	AvgSim(↑)	ASR(↑)	AvgSim(↑)
AnyAttack	1.62	0.0830	1.76	0.0765	1.52	0.0810	1.98	0.0880	1.72	0.0821
CoA	1.60	0.0828	2.04	0.0879	2.14	0.0876	1.68	0.0897	1.87	0.0870
M-Attack	3.48	0.1046	13.80	0.1915	25.66	0.3028	13.36	0.2048	14.08	0.2009
FOA-Attack	3.62	0.1071	14.34	0.2042	28.28	0.3191	15.38	0.2198	15.41	0.2126
MPCAttack	5.24	0.1228	33.24	0.3338	46.30	0.4174	33.38	0.3364	29.54	0.3026
Untargeted	Victim Black-box Open-Source Models									
	Qwen2.5-VL-7B		InternVL3-8B		LLaVa-1.5-7B		GLM-4.1V-9B-Thinking		Average	
	ASR(↑)	AvgSim(↓)	ASR(↑)	AvgSim(↓)	ASR(↑)	AvgSim(↓)	ASR(↑)	AvgSim(↓)	ASR(↑)	AvgSim(↓)
AnyAttack	35.20	0.5255	18.60	0.6281	27.66	0.5622	24.60	0.5876	26.52	0.5759
CoA	32.55	0.5372	19.48	0.6159	29.5	0.5570	19.69	0.6093	25.28	0.5799
X-Transfer	42.84	0.4499	46.54	0.4444	49.20	0.4170	35.74	0.5117	43.58	0.4558
M-Attack	21.02	0.6098	35.36	0.5280	75.28	0.2835	38.64	0.4974	42.58	0.4797
FOA-Attack	22.22	0.6048	37.26	0.5148	77.20	0.2623	43.24	0.4747	44.98	0.4642
MPCAttack	32.14	0.5447	63.00	0.3511	92.52	0.1442	68.28	0.3171	63.99	0.3393

Table 4. Performance of ASR (%) and AvgSim on closed-source MLLMs across both targeted and untargeted settings on Flickr30K dataset.

Targeted	Victim Black-box Closed-Source Models									
	GPT-4o		GPT-5		Claude-3.5		Gemini-2.0		Average	
	ASR(↑)	AvgSim(↑)	ASR(↑)	AvgSim(↑)	ASR(↑)	AvgSim(↑)	ASR(↑)	AvgSim(↑)	ASR(↑)	AvgSim(↑)
AnyAttack	1.36	0.0764	1.28	0.0757	1.78	0.0671	1.60	0.0766	1.51	0.0739
CoA	1.84	0.0801	1.86	0.0809	1.58	0.0726	1.92	0.0810	1.80	0.0787
M-Attack	9.72	0.1667	9.82	0.1678	8.88	0.1528	5.00	0.1209	8.35	0.1521
FOA-Attack	10.22	0.1717	11.66	0.1855	11.70	0.1686	5.54	0.1232	9.78	0.1623
MPCAttack	23.22	0.2674	24.78	0.2756	15.46	0.2017	12.90	0.1844	19.09	0.2323
Untargeted	Victim Black-box Closed-Source Models									
	GPT-4o		GPT-5		Claude-3.5		Gemini-2.0		Average	
	ASR(↑)	AvgSim(↓)	ASR(↑)	AvgSim(↓)	ASR(↑)	AvgSim(↓)	ASR(↑)	AvgSim(↓)	ASR(↑)	AvgSim(↓)
AnyAttack	16.92	0.6356	14.36	0.6545	55.42	0.3953	14.74	0.6517	25.36	0.5843
CoA	19.54	0.6220	15.66	0.6394	51.40	0.4348	14.64	0.6536	25.31	0.5875
X-Transfer	47.24	0.4390	38.74	0.4920	64.66	0.3437	37.02	0.5111	46.91	0.4465
M-Attack	36.60	0.5205	36.40	0.5210	51.60	0.4316	18.68	0.6251	35.82	0.5246
FOA-Attack	38.38	0.5040	32.78	0.5371	53.64	0.4206	19.48	0.6237	36.07	0.5214
MPCAttack	61.84	0.3576	54.50	0.4009	65.22	0.3399	38.00	0.5096	54.89	0.4020

ilarity between the target response and the adversarial response is measured. The resulting similarity score is then compared with a predefined threshold to determine whether the attack is successful. When ground-truth responses are available for the source and target images, these reference answers can be used instead of the model-generated responses to provide a more reliable reference, yielding a more accurate assessment of adversarial effectiveness.

4. Experiments

4.1. Experimental Setting

Datasets. Following [25, 29], we adopt 1,000 images from the ImageNet [9] subset used in the NIPS 2017 Adversarial Attacks and Defenses Competition. To further evaluate the generalization capability of our method across different domains, we conduct experiments on two widely used multimodal benchmarks: Flickr30K [36] and MME [4].

The Flickr30K dataset comprises approximately 31,783 images collected from Flickr, each annotated with five human-written natural language descriptions. We select 1,000 images and their corresponding captions as source–target pairs for evaluation. The MME dataset serves as a comprehensive benchmark for assessing the multi-modal understanding ability of large language models, where each sample involves yes/no questions designed to directly reflect the factual correctness of model responses.

Victim black-box models. We evaluate the transferability of adversarial examples on both open-source and closed-source MLLMs. The open-source models include Qwen2.5-VL-7B, InternVL3-8B, LLaVA-1.5-7B, and GLM-4.1V-9B-Thinking. All open-source MLLMs are evaluated using the VLMEvalKit [12] toolkit to ensure consistency. The closed-source models include GPT-4o, GPT-5, Claude-3.5, and Gemini-2.0. For these models, the text

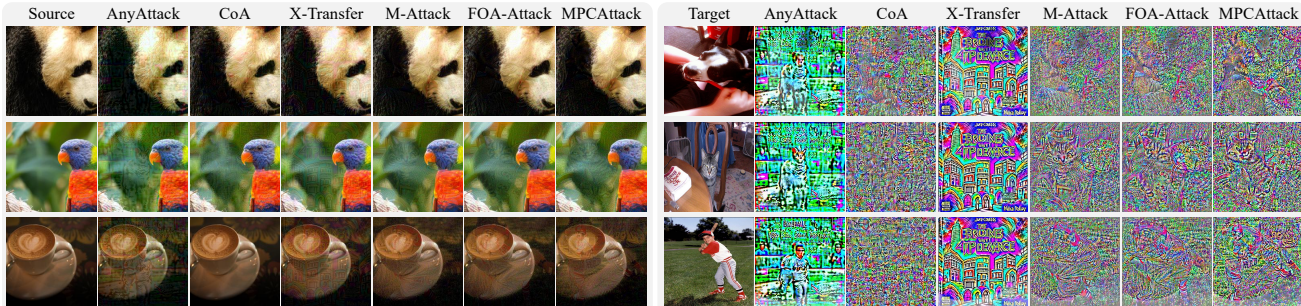


Figure 3. Visualization of adversarial images and perturbations.

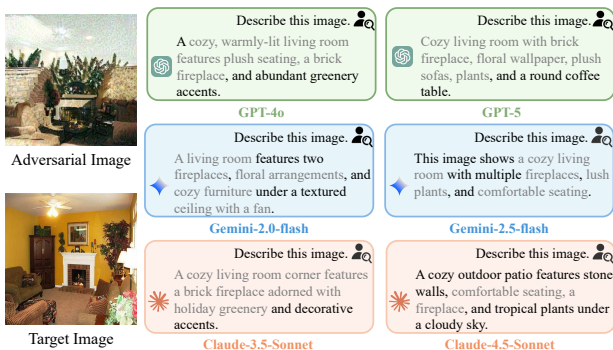


Figure 4. Adversarial examples generated by MPCAttack, with responses from closed-source MLLMs.

prompt of these models is set to “Describe this image in one concise sentence, no longer than 20 words.”

Baselines. We compare the MPCAttack with five advanced transferable adversarial attack methods for MLLMs, including AnyAttack [50], CoA [48], X-Transfer [23], M-Attack [29], and FOA-Attack [25]. All methods follow their original settings to generate adversarial examples.

Implementation details. We adopt CLIP [37], InternVL3-1B [53], and DINOv2 [34] as the surrogate models for the cross-modal alignment paradigm, multi-modal understanding paradigm, and visual self-supervised paradigm, respectively. The perturbation budget is set to $\epsilon = 16/255$ under the ℓ_∞ -norm constraint, with an attack step size of $1/255$ and a total of 300 optimization iterations. The weighting factor λ is set to 0.6, the temperature coefficient τ for \mathcal{L} is set to 0.2, and the balance coefficient ω is set to 2. All experiments are conducted on a single NVIDIA RTX 3090 GPU.

Evaluation metrics. Following [25], we adopt the widely recognized LLM-as-a-judge framework for evaluation. Specifically, we employ the same victim model to generate textual descriptions for the source, target, and adversarial images, and then compute their semantic similarity using GPTScore. If the dataset provides ground-truth

captions (e.g., Flickr30K), these captions are used as textual references. For targeted attacks, an attack is considered successful when the similarity score between the adversarial image and the target image exceeds threshold (0.5), indicating that they convey the same semantic content. For untargeted attacks, success is determined when the similarity score between the adversarial image and the source image falls below threshold (0.5), suggesting that the adversarial example no longer preserves the semantic meaning of the source image. Comprehensive evaluation prompts and additional implementation details are provided in the supplementary material.

4.2. Experimental Results

We evaluate various transferable attack methods on multiple open-source and closed-source MLLMs, with results summarized in Table 1 and Table 2. MPCAttack consistently achieves the highest attack success rate (ASR) and semantic similarity (AvgSim) across both targeted and untargeted settings, demonstrating its superior transferability. On open-source models, it achieves an ASR of 63.33% in the targeted setting, substantially outperforming existing methods. In the untargeted scenario, MPCAttack further boosts ASR to 92.10%, indicating stronger attack efficacy and semantic deviation. Its effectiveness extends to closed-source models, highlighting remarkable generalization. By contrast, methods such as CoA show limited transferability due to reliance on a lightweight single-paradigm model, making MPCAttack the robust and generalizable approach for generating transferable adversarial examples.

Table 3 and Table 4 report MPCAttack’s results on the Flickr30K dataset, further validating its robustness across datasets. On open-source models, MPCAttack achieves a targeted ASR of 29.54%, significantly surpassing FOA-Attack (15.41%). In the untargeted setting, it attains 63.99% ASR, demonstrating strong attack success and semantic deviation. Notably, the overall ASR on the Flickr30K dataset is relatively low. This may be attributed to the fact that each image in Flickr30K is associated with five captions, each describing the image from different per-

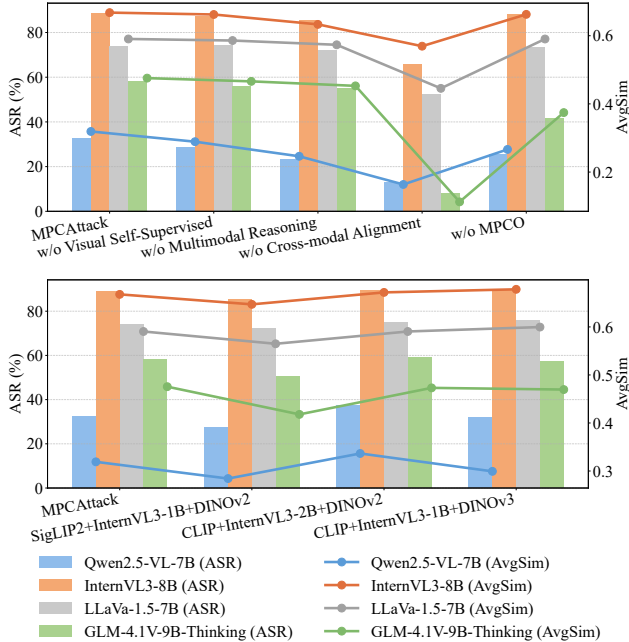


Figure 5. Ablation study for different learning paradigms and MPCO strategy.

spectives. Consequently, MLLMs-generated descriptions may not comprehensively capture all semantic aspects of images, leading to a reduced ASR. Figure 3 illustrates the adversarial examples and perturbations generated by different methods, showing that the perturbations produced by MPCAttack better capture the characteristics of the target images. Figure 4 presents examples of MPCAttack successfully misleading closed-source MLLMs in their responses. These results demonstrate MPCAttack’s ability to generate globally optimized, highly transferable adversarial perturbations, advancing multimodal security research. More results on the MME dataset and visualization are provided in the supplementary material.

4.3. Ablation Study

Impact of multi-paradigm collaboration. Figure 5 presents the contribution of each learning paradigm to MPCAttack’s transferability. Removing any component consistently reduces ASR and AvgSim, verifying that all modules are indispensable. Notably, excluding the cross-modal alignment paradigm leads to the most significant degradation, highlighting its central role due to the strong alignment between MLLM visual encoders and cross-modal representations. Removing MPCO also markedly weakens performance, particularly on challenging models such as GLM-4.1V-9B-Thinking, demonstrating its importance for multi-paradigm feature aggregation and global optimization. We further examine the influence of specific backbone models. Replacing CLIP with SigLIP2 [44] decreases transfer-

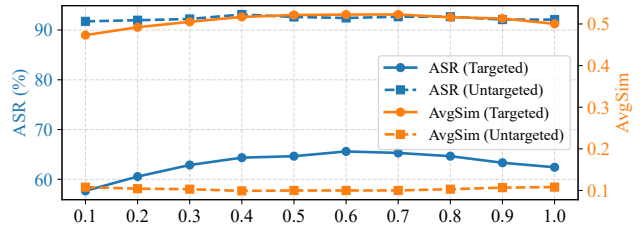


Figure 6. Impact of weighting factor λ .

ability, whereas substituting InternVL3-1B with the larger InternVL3-2B improves it, indicating that CLIP provides stronger transferable adversarial signals and that larger multimodal models enhance transferability at increased computational cost. The performance gap between DINOv2 and DINOv3 [40] is marginal.

Impact of weighting factor λ . Figure 6 shows the average attack performance of MPCAttack under different values of λ on open-source MLLMs, which controls the fusion ratio between image and text features extracted from the cross-modal alignment model. This parameter balances the contributions of visual and linguistic semantics in the joint feature representation. When λ is too small, the model over-relies on text features, resulting in insufficient visual representation and adversarial perturbations that miss fine-grained visual details. Conversely, a too-large λ emphasizes image features, reducing semantic consistency and causing an imbalance in the cross-modal representation. An intermediate λ achieves an optimal trade-off, producing adversarial examples with stronger transferability. Notably, $\lambda = 1$ (image-only features) does not attain optimal performance, indicating that relying solely on the visual modality cannot fully capture the critical semantic information in images, limiting the semantic consistency and transferability of adversarial examples.

5. Conclusion

In this paper, we proposed MPCAttack, a novel transferable adversarial attack framework that jointly optimizes multi-paradigm feature representations to generate adversarial examples against MLLMs. By collaboratively aggregating features from cross-modal alignment, multi-modal understanding, and visual self-supervised learning paradigms, MPCAttack achieves a unified global optimization that produces more semantically consistent and highly transferable perturbations. Extensive experiments on both open-source and closed-source MLLMs demonstrate that our method consistently achieves superior attack performance compared to SOTA approaches. These findings reveal the persistent vulnerabilities within current MLLMs and highlight the crucial role of MPCAttack in designing more effective and transferable adversarial examples.

6. Acknowledgement

This work is supported in part by the National Key Research and Development Program of China (2023YFE0116300, 2023YFF1105102, 2023YFF1105105), the National Natural Science Foundation of China (62020106012, 62332008, 62336004, U1836218, 62106089, 62202205), the 111 Project of Ministry of Education of China (B12018), and the Engineering and Physical Sciences Research Council (EP-SRC) (EP/V002856/1).

References

- [1] Josh Achiam, Steven Adler, Sandhini Agarwal, Lama Ahmad, Ilge Akkaya, Florencia Leoni Aleman, Diogo Almeida, Janko Altenschmidt, Sam Altman, Shyamal Anadkat, et al. Gpt-4 technical report. *arXiv preprint arXiv:2303.08774*, 2023. 1
- [2] Shuai Bai, Keqin Chen, Xuejing Liu, Jialin Wang, Wenbin Ge, Sibao Song, Kai Dang, Peng Wang, Shijie Wang, Jun Tang, et al. Qwen2. 5-vl technical report. *arXiv preprint arXiv:2502.13923*, 2025. 1, 3
- [3] Mathilde Caron, Hugo Touvron, Ishan Misra, Hervé Jégou, Julien Mairal, Piotr Bojanowski, and Armand Joulin. Emerging properties in self-supervised vision transformers. In *Proceedings of the IEEE/CVF international conference on computer vision*, pages 9650–9660, 2021. 3
- [4] Fu Chaoyou, Chen Peixian, Shen Yunhang, Qin Yulei, Zhang Mengdan, Lin Xu, Yang Jinrui, Zheng Xiawu, Li Ke, Sun Xing, et al. Mmc: A comprehensive evaluation benchmark for multimodal large language models. *arXiv preprint arXiv:2306.13394*, 3, 2023. 6
- [5] Huanran Chen, Yichi Zhang, Yinpeng Dong, Xiao Yang, Hang Su, and Jun Zhu. Rethinking model ensemble in transfer-based adversarial attacks. In *The Twelfth International Conference on Learning Representations*, 2024. 2
- [6] Jun Chen, Han Guo, Kai Yi, Boyang Li, and Mohamed Elhoseiny. Visualgpt: Data-efficient adaptation of pretrained language models for image captioning. In *Proceedings of the IEEE/CVF conference on computer vision and pattern recognition*, pages 18030–18040, 2022. 3
- [7] Zhe Chen, Jiannan Wu, Wenhai Wang, Weijie Su, Guo Chen, Sen Xing, Muyan Zhong, Qinglong Zhang, Xizhou Zhu, Lewei Lu, et al. Internvl: Scaling up vision foundation models and aligning for generic visual-linguistic tasks. In *Proceedings of the IEEE/CVF conference on computer vision and pattern recognition*, pages 24185–24198, 2024. 3
- [8] Gheorghe Comanici, Eric Bieber, Mike Schaekermann, Ice Pasupat, Noveen Sachdeva, Inderjit Dhillon, Marcel Blstein, Ori Ram, Dan Zhang, Evan Rosen, et al. Gemini 2.5: Pushing the frontier with advanced reasoning, multimodality, long context, and next generation agentic capabilities. *arXiv preprint arXiv:2507.06261*, 2025. 3
- [9] Jia Deng, Wei Dong, Richard Socher, Li-Jia Li, Kai Li, and Li Fei-Fei. Imagenet: A large-scale hierarchical image database. In *2009 IEEE conference on computer vision and pattern recognition*, pages 248–255. Ieee, 2009. 6
- [10] Yinpeng Dong, Fangzhou Liao, Tianyu Pang, Hang Su, Jun Zhu, Xiaolin Hu, and Jianguo Li. Boosting adversarial attacks with momentum. In *Proceedings of the IEEE conference on computer vision and pattern recognition*, pages 9185–9193, 2018. 2
- [11] Yinpeng Dong, Huanran Chen, Jiawei Chen, Zhengwei Fang, Xiao Yang, Yichi Zhang, Yu Tian, Hang Su, and Jun Zhu. How robust is google’s bard to adversarial image attacks? *arXiv preprint arXiv:2309.11751*, 2023. 2
- [12] Haodong Duan, Junming Yang, Yuxuan Qiao, Xinyu Fang, Lin Chen, Yuan Liu, Xiaoyi Dong, Yuhang Zang, Pan Zhang, Jiaqi Wang, et al. Vlmevalkit: An open-source toolkit for evaluating large multi-modality models. In *Proceedings of the 32nd ACM international conference on multimedia*, pages 11198–11201, 2024. 6
- [13] Qianhan Feng, Wenshuo Li, Tong Lin, and Xinghao Chen. Align-kd: Distilling cross-modal alignment knowledge for mobile vision-language large model enhancement. In *Proceedings of the Computer Vision and Pattern Recognition Conference*, pages 4178–4188, 2025. 3
- [14] Zheren Fu, Lei Zhang, Hou Xia, and Zhendong Mao. Linguistic-aware patch slimming framework for fine-grained cross-modal alignment. In *Proceedings of the IEEE/CVF Conference on Computer Vision and Pattern Recognition*, pages 26307–26316, 2024. 3
- [15] Sensen Gao, Xiaojun Jia, Xuhong Ren, Ivor Tsang, and Qing Guo. Boosting transferability in vision-language attacks via diversification along the intersection region of adversarial trajectory. In *European Conference on Computer Vision*, pages 442–460. Springer, 2024. 2
- [16] Ian J Goodfellow, Jonathon Shlens, and Christian Szegedy. Explaining and harnessing adversarial examples. *arXiv preprint arXiv:1412.6572*, 2014. 2
- [17] Jie Gui, Tuo Chen, Jing Zhang, Qiong Cao, Zhenan Sun, Hao Luo, and Dacheng Tao. A survey on self-supervised learning: Algorithms, applications, and future trends. *IEEE Transactions on Pattern Analysis and Machine Intelligence*, 46(12):9052–9071, 2024. 3
- [18] Qi Guo, Shanmin Pang, Xiaojun Jia, Yang Liu, and Qing Guo. Efficient generation of targeted and transferable adversarial examples for vision-language models via diffusion models. *IEEE Transactions on Information Forensics and Security*, 20:1333–1348, 2024. 2
- [19] Kaiming He, Xinlei Chen, Saining Xie, Yanghao Li, Piotr Dollár, and Ross Girshick. Masked autoencoders are scalable vision learners. In *Proceedings of the IEEE/CVF conference on computer vision and pattern recognition*, pages 16000–16009, 2022. 3
- [20] Wenyi Hong, Weihang Wang, Qingsong Lv, Jiazheng Xu, Wenmeng Yu, Junhui Ji, Yan Wang, Zihan Wang, Yuxiao Dong, Ming Ding, et al. Cogagent: A visual language model for gui agents. In *Proceedings of the IEEE/CVF Conference on Computer Vision and Pattern Recognition*, pages 14281–14290, 2024. 3
- [21] Xiaowei Hu, Zhe Gan, Jianfeng Wang, Zhengyuan Yang, Zicheng Liu, Yumao Lu, and Lijuan Wang. Scaling up vision-language pre-training for image captioning. In *Pro-*

- ceedings of the *IEEE/CVF conference on computer vision and pattern recognition*, pages 17980–17989, 2022. 3
- [22] Hailang Huang, Zhijie Nie, Ziqiao Wang, and Ziyu Shang. Cross-modal and uni-modal soft-label alignment for image-text retrieval. In *Proceedings of the AAAI Conference on Artificial Intelligence*, pages 18298–18306, 2024. 3
- [23] Hanxun Huang, Sarah Monazam Erfani, Yige Li, Xingjun Ma, and James Bailey. X-transfer attacks: Towards super transferable adversarial attacks on clip. In *Forty-second International Conference on Machine Learning*, 2025. 2, 7
- [24] Xiaojun Jia, Sensen Gao, Qing Guo, Simeng Qin, Ke Ma, Yihao Huang, Yang Liu, Ivor W. Tsang, and Xiaochun Cao. Semantic-aligned adversarial evolution triangle for high-transferability vision-language attack. *IEEE Transactions on Pattern Analysis and Machine Intelligence*, 47(10): 8489–8505, 2025. 2
- [25] Xiaojun Jia, Sensen Gao, Simeng Qin, Tianyu Pang, Chao Du, Yihao Huang, Xinfeng Li, Yiming Li, Bo Li, and Yang Liu. Adversarial attacks against closed-source mllms via feature optimal alignment. *arXiv preprint arXiv:2505.21494*, 2025. 1, 2, 3, 6, 7
- [26] Dehong Kong, Siyuan Liang, Xiaopeng Zhu, Yuansheng Zhong, and Wenqi Ren. Patch is enough: naturalistic adversarial patch against vision-language pre-training models. *Visual Intelligence*, 2(1):33, 2024. 2
- [27] Yuanbo Li, Cong Hu, Rui Wang, and Xiaojun Wu. Hierarchical feature transformation attack: Generate transferable adversarial examples for face recognition. *Applied Soft Computing*, 172:112823, 2025. 2
- [28] Yuanbo Li, Cong Hu, and Xiao-Jun Wu. Transferable stealthy adversarial example generation via dual-latent adaptive diffusion for facial privacy protection. *IEEE Transactions on Information Forensics and Security*, 20:9427–9440, 2025. 2
- [29] Zhaoyi Li, Xiaohan Zhao, Dong-Dong Wu, Jiacheng Cui, and Zhiqiang Shen. A frustratingly simple yet highly effective attack baseline: Over 90% success rate against the strong black-box models of gpt-4.5/4o/o1. In *ICML 2025 Workshop on Reliable and Responsible Foundation Models*, 2025. 2, 3, 6, 7, 1
- [30] Haotian Liu, Chunyuan Li, Qingyang Wu, and Yong Jae Lee. Visual instruction tuning. *Advances in neural information processing systems*, 36:34892–34916, 2023. 3
- [31] Haotian Liu, Chunyuan Li, Yuheng Li, and Yong Jae Lee. Improved baselines with visual instruction tuning. In *Proceedings of the IEEE/CVF Conference on Computer Vision and Pattern Recognition (CVPR)*, pages 26296–26306, 2024. 3
- [32] Xiyao Liu, Jiabin Hu, Qingying Yang, Ming Jiang, Jianbiao He, and Hui Fang. A divide-and-conquer reconstruction method for defending against adversarial example attacks. *Visual Intelligence*, 2(1):30, 2024. 2
- [33] Duc-Tuan Luu, Viet-Tuan Le, and Duc Minh Vo. Questioning, answering, and captioning for zero-shot detailed image caption. In *Proceedings of the Asian Conference on Computer Vision*, pages 242–259, 2024. 3
- [34] Maxime Oquab, Timothée Darcet, Théo Moutakanni, Huy Vo, Marc Szafraniec, Vasil Khalidov, Pierre Fernandez, Daniel Haziza, Francisco Massa, Alaaeldin El-Nouby, et al. Dinov2: Learning robust visual features without supervision. *Transactions on Machine Learning Research Journal*, pages 1–31, 2024. 2, 3, 7
- [35] Övgü Özdemir and Erdem Akagündüz. Enhancing visual question answering through question-driven image captions as prompts. In *Proceedings of the IEEE/CVF Conference on Computer Vision and Pattern Recognition*, pages 1562–1571, 2024. 3
- [36] Bryan A Plummer, Liwei Wang, Chris M Cervantes, Juan C Caicedo, Julia Hockenmaier, and Svetlana Lazebnik. Flickr30k entities: Collecting region-to-phrase correspondences for richer image-to-sentence models. In *Proceedings of the IEEE international conference on computer vision*, pages 2641–2649, 2015. 6
- [37] Alec Radford, Jong Wook Kim, Chris Hallacy, Aditya Ramesh, Gabriel Goh, Sandhini Agarwal, Girish Sastry, Amanda Askell, Pamela Mishkin, Jack Clark, et al. Learning transferable visual models from natural language supervision. In *International conference on machine learning*, pages 8748–8763. Pmlr, 2021. 2, 3, 7
- [38] Yuchen Ren, Zhengyu Zhao, Chenhao Lin, Bo Yang, Lu Zhou, Zhe Liu, and Chao Shen. Improving adversarial transferability on vision transformers via forward propagation refinement. In *Proceedings of the Computer Vision and Pattern Recognition Conference*, pages 25071–25080, 2025. 2
- [39] Christian Schlarman and Matthias Hein. On the adversarial robustness of multi-modal foundation models. In *Proceedings of the IEEE/CVF International Conference on Computer Vision*, pages 3677–3685, 2023. 2
- [40] Oriane Siméoni, Huy V Vo, Maximilian Seitzer, Federico Baldassarre, Maxime Oquab, Cijo Jose, Vasil Khalidov, Marc Szafraniec, Seungeun Yi, Michaël Ramamonjisoa, et al. Dinov3. *arXiv preprint arXiv:2508.10104*, 2025. 3, 8
- [41] Quan Sun, Yuxin Fang, Ledell Wu, Xinlong Wang, and Yue Cao. Eva-clip: Improved training techniques for clip at scale. *arXiv preprint arXiv:2303.15389*, 2023. 3
- [42] Gemini Team, Rohan Anil, Sebastian Borgeaud, Jean-Baptiste Alayrac, Jiahui Yu, Radu Soricut, Johan Schalkwyk, Andrew M Dai, Anja Hauth, Katie Millican, et al. Gemini: a family of highly capable multimodal models. *arXiv preprint arXiv:2312.11805*, 2023. 3
- [43] Michael Tschannen, Manoj Kumar, Andreas Steiner, Xiaohua Zhai, Neil Houlsby, and Lucas Beyer. Image captioners are scalable vision learners too. *Advances in Neural Information Processing Systems*, 36:46830–46855, 2023. 3
- [44] Michael Tschannen, Alexey Gritsenko, Xiao Wang, Muhammad Ferjad Naeem, Ibrahim Alabdulmohsin, Nikhil Parthasarathy, Talfan Evans, Lucas Beyer, Ye Xia, Basil Mustafa, et al. Siglip 2: Multilingual vision-language encoders with improved semantic understanding, localization, and dense features. *arXiv preprint arXiv:2502.14786*, 2025. 3, 8
- [45] Weihang Wang, Qingsong Lv, Wenmeng Yu, Wenyi Hong, Ji Qi, Yan Wang, Junhui Ji, Zhuoyi Yang, Lei Zhao, Song XiXuan, et al. CogVlm: Visual expert for pretrained language

- models. *Advances in Neural Information Processing Systems*, 37:121475–121499, 2024. [1](#)
- [46] Chengyue Wu, Xiaokang Chen, Zhiyu Wu, Yiyang Ma, Xingchao Liu, Zizheng Pan, Wen Liu, Zhenda Xie, Xingkai Yu, Chong Ruan, et al. Janus: Decoupling visual encoding for unified multimodal understanding and generation. In *Proceedings of the Computer Vision and Pattern Recognition Conference*, pages 12966–12977, 2025. [3](#)
- [47] Jiannan Wu, Muyan Zhong, Sen Xing, Zeqiang Lai, Zhaoyang Liu, Zhe Chen, Wenhai Wang, Xizhou Zhu, Lewei Lu, Tong Lu, et al. Visionllm v2: An end-to-end generalist multimodal large language model for hundreds of vision-language tasks. *Advances in Neural Information Processing Systems*, 37:69925–69975, 2024. [3](#)
- [48] Peng Xie, Yequan Bie, Jianda Mao, Yangqiu Song, Yang Wang, Hao Chen, and Kani Chen. Chain of attack: On the robustness of vision-language models against transfer-based adversarial attacks. In *Proceedings of the Computer Vision and Pattern Recognition Conference*, pages 14679–14689, 2025. [1](#), [2](#), [7](#)
- [49] Ziyi Yin, Muchao Ye, Tianrong Zhang, Tianyu Du, Jinguo Zhu, Han Liu, Jinghui Chen, Ting Wang, and Fenglong Ma. Vlattack: Multimodal adversarial attacks on vision-language tasks via pre-trained models. *Advances in Neural Information Processing Systems*, 36:52936–52956, 2023. [2](#)
- [50] Jiaming Zhang, Junhong Ye, Xingjun Ma, Yige Li, Yunfan Yang, Yunhao Chen, Jitao Sang, and Dit-Yan Yeung. Anyattack: Towards large-scale self-supervised adversarial attacks on vision-language models. In *Proceedings of the Computer Vision and Pattern Recognition Conference*, pages 19900–19909, 2025. [2](#), [7](#)
- [51] Yunqing Zhao, Tianyu Pang, Chao Du, Xiao Yang, Chongxuan Li, Ngai-Man Man Cheung, and Min Lin. On evaluating adversarial robustness of large vision-language models. *Advances in Neural Information Processing Systems*, 36:54111–54138, 2023. [2](#)
- [52] Deyao Zhu, Jun Chen, Xiaoqian Shen, Xiang Li, and Mohamed Elhoseiny. Minigpt-4: Enhancing vision-language understanding with advanced large language models. In *The Twelfth International Conference on Learning Representations*, 2024. [1](#)
- [53] Jinguo Zhu, Weiyun Wang, Zhe Chen, Zhaoyang Liu, Shenglong Ye, Lixin Gu, Hao Tian, Yuchen Duan, Weijie Su, Jie Shao, et al. Internvl3: Exploring advanced training and test-time recipes for open-source multimodal models. *arXiv preprint arXiv:2504.10479*, 2025. [3](#), [7](#)

Multi-Paradigm Collaborative Adversarial Attack Against Multi-Modal Large Language Models

Supplementary Material

In this supplementary material, we provide the algorithm of the proposed MPCAttack, a detailed description of the dataset and evaluation prompt, the experimental results on the MME dataset, the ablation experiments for Multi-Paradigm, the parameter experiments of the loss function, and the visualization of the attack on adversarial examples on closed-source MLLMs.

7. A Detailed Algorithm of MPCAttack

The detailed description of the proposed MPCAttack is shown in Algorithm 1.

8. Detailed Datasets and Evaluation Prompt

ImageNet. The ImageNet dataset, which is the most commonly used dataset in the field of adversarial attacks, we adopt 1,000 images from the ImageNet subset used in the NIPS 2017 Adversarial Attacks and Defenses Competition following [25, 29].

Flickr30K. The Flickr30K dataset contains approximately 31,783 images collected from Flickr, and each image is accompanied by five natural language descriptions written by humans. As a commonly used multimodal dataset, it has ground truth captions. Therefore, we randomly select 1000 images along with their corresponding captions. During the generation of adversarial examples, we sequentially select source images and select target images in reverse order to produce the adversarial examples. During the evaluation phase, we directly use the ground truth captions as the source and target descriptions to compute similarity scores with the adversarial descriptions.

MME. The MME dataset provides a comprehensive benchmark for evaluating the multimodal understanding capabilities of large language models, where each sample contains a yes/no type question designed to directly reflect the accuracy of the model’s responses. It comprises 1,187 images, each paired with two questions corresponding to “yes” and “no” answers. During the generation of adversarial examples, we sequentially select source images and select target images in reverse order to produce the adversarial examples. During the evaluation phase, for targeted attacks, the adversarial examples are paired with the target image’s question and fed into the victim black-box MLLMs, which provide a yes or no answer; the attack is considered successful if the model’s response indicates misclassification. For untargeted attacks, the adversarial examples are paired with the source image’s question and similarly evaluated against the

Algorithm 1 MPCAttack

Input: Source image x_s , target image x_t , multi-paradigm image encoders f_{c_I}, f_m, f_v , multi-modal understanding text generator f_{mg} , cross-modal alignment text encoder f_{c_T} , loss function \mathcal{L} , weighting factor λ , image processing \mathcal{T} , perturbation budget ϵ , iterations N , step size α , momentum factor μ .

Output: Adversarial image x_{adv} .

- 1: Initialize: $x_{adv}^0 = x_s + \delta^0, g^0 = 0$; // Initialize adversarial image x_{adv} with random noise δ^0
 - 2: **for** $n = 0$ to $N - 1$ **do**
 - 3: $\hat{x}_{adv}^n = \mathcal{T}(x_{adv}^n)$; // Perform random crop
 - 4: Get multi-paradigm aggregated features z_{adv}, z_s, z_t from $\hat{x}_{adv}^n, x_s, x_t$ by Eq. (2), (3), (4), (5);
 - 5: Compute loss \mathcal{L} by Eq. (6);
 - 6: $g^{n+1} = \mu \cdot g^n + \frac{\nabla \mathcal{L}}{\|\nabla \mathcal{L}\|}$;
 - 7: $\delta^{n+1} = \text{Clip}(\delta^n + \alpha \cdot \text{sign}(g^{n+1}), -\epsilon, \epsilon)$;
 - 8: $x_{adv}^{n+1} = x_{adv}^n + \delta^{n+1}$
 - 9: **end for**
 - 10: **return** $x_{adv} = x_{adv}^N$
-

victim black-box MLLMs. Notably, we only use the question corresponding to the “yes” answer for evaluation, as in practice we found that the “no” question often does not correspond to the associated image, making it incapable of reliably reflecting whether the adversarial sample successfully succeeds and thus unsuitable for a proper assessment.

Evaluation prompt. Following [25], we adopt the same way to evaluate the adversarial performance. Below is the detailed evaluation prompt used to assess semantic similarity between textual inputs. The “{text1}” and “{text2}” are used as placeholders for text inputs. The evaluation prompt template is shown in Figure 7.

9. Detailed Models

Table 5 lists the models used by each paradigm. Here, “main” indicates the primary model used, while “ablation” represents the other models employed in the ablation study in Figure 5. Because the current commonly used image encoders of MLLMs tend to be pre-trained models that are trained using the cross-modal alignment paradigm. Therefore, we mainly adopt the CLIP framework as the main paradigm and integrate three different-sized CLIP models.

Evaluation Prompt

Rate the semantic similarity between the following two texts on a scale from 0 to 1.

Criteria for similarity measurement:

- Main Subject Consistency:** If both descriptions refer to the same key subject or object (e.g., a person, food, an event), they should receive a higher similarity score.
- Relevant Description:** If the descriptions are related to the same context or topic, they should also contribute to a higher similarity score.
- Ignore Fine-Grained Details:** Do not penalize differences in phrasing, sentence structure, or minor variations in detail. Focus on whether both descriptions fundamentally describe the same thing.
- Partial Matches:** If one description contains extra information but does not contradict the other, they should still have a high similarity score.
- Similarity Score Range:**
 - 1.0:** Nearly identical in meaning.
 - 0.8-0.9:** Same subject, with highly related descriptions.
 - 0.7-0.8:** Same subject, core meaning aligned, even if some details differ.
 - 0.5-0.7:** Same subject but different perspectives or missing details.
 - 0.3-0.5:** Related but not highly similar (same general theme but different descriptions).
 - 0.0-0.2:** Completely different subjects or unrelated meanings.

Text 1: {text1}

Text 2: {text2}

Output only a single number between 0 and 1. Do not include any explanation or additional text.

Figure 7. Evaluation prompt template.

Table 5. The models used by each paradigm.

Cross-Modal Alignment Paradigm	clip-vit-base-patch16 (main) clip-vit-base-patch32 (main) CLIP-ViT-G-14-laion2B-s12B-b42K (main) siglip2-base-patch16-224 (ablation) siglip2-base-patch32-256 (ablation) siglip2-giant-opt-patch16-256 (ablation)
Multimodal Understanding Paradigm	InternVL3-1B (main) InternVL3-2B (ablation)
Visual Self-Supervised Paradigm	dinov2-base(main) dinov3-base (ablation)

10. Experimental Results on MME dataset

Tables 6 and 7 present the attack success rates of different methods on both open-source and closed-source MLLMs. Across all settings, MPCAttack consistently delivers the highest ASR, demonstrating strong generalization in both targeted and untargeted attack scenarios. On open-source MLLMs, MPCAttack yields clear performance gains, particularly on InternVL3-8B and glm-4.1v-9b-thinking, where it surpasses FOA-Attack by large margins in both attack types. Its average ASR improves by 5.90% in targeted and 9.29% in untargeted settings, confirming the effectiveness of multi-paradigm collaborative optimization. On closed-source MLLMs, the superiority of MPCAttack is even more pronounced. It achieves the highest ASR on all models, outperforming FOA-Attack by 5.35% (targeted) and 6.22% (untargeted) on average. The improvements on challenging models such as GPT-

5 and Claude-4.5 indicate stronger transferability to unseen architectures with distinct training pipelines. The results demonstrate that MPCAttack enhances attack transferability across diverse model families, highlighting the advantage of aggregating multi-paradigm representations for globally optimized adversarial perturbations.

11. Attack performance under defense mechanisms and diverse settings

We evaluate our method under representative defense strategies (e.g., DiffPure) as well as diverse input conditions (e.g., additive noise). As shown in Table 8, MPCAttack largely preserves its attack effectiveness under these challenging settings. Moreover, compared with M-Attack and FOA-Attack, MPCAttack exhibits significantly less performance degradation when facing defense mechanisms and environmental variations, demonstrating its superior robustness.

12. Ablation Study for Multi-Paradigm

The results in Table 9 clearly demonstrate the effectiveness of incorporating the Multi-Paradigm mechanism. For both M-Attack and FOA-Attack, adding the Multi-Paradigm module consistently improves ASR and semantic similarity across all victim models in both targeted and untargeted settings. These gains indicate that integrating complementary paradigm-specific representations can enrich gradient signals and provide more coherent optimization guidance, thereby enhancing the overall attack strength. However, despite these improvements, the Multi-Paradigm-enhanced

variants still fall short of MPCAttack. This gap highlights an important limitation of directly extending existing methods: although they benefit from additional paradigms, their optimization remains largely independent across feature types. Such optimization can lead to redundant gradient directions, restricting their ability to fully leverage complementary information. In contrast, MPCAttack jointly optimizes multi-paradigm features in a unified framework, enabling coordinated gradient alignment and globally consistent perturbation updates. This integrated optimization yields more effective and transferable adversarial perturbations, outperforming all baselines by a clear margin.

13. Analysis of Loss-Function Parameter Effects

Since the loss function \mathcal{L} contains two parameters, where τ is a temperature coefficient that controls the sharpness of the similarity distribution, and ω is a balancing factor that regulates the trade-off between positive pairs and negative pairs. Table 10 evaluates the influence of the temperature coefficient τ and the balancing factor ω in the loss function. As τ controls the sharpness of the similarity distribution, overly small values lead to unstable optimization and poor ASR, while excessively large values oversmooth the distribution and weaken contrastive guidance. Moderate values (e.g., $\tau=0.2-0.4$) achieve the best balance and yield consistently strong performance. Meanwhile, ω regulates the trade-off between positive and negative pairs: small values overemphasize source separation and hinder targeted alignment, whereas overly large values bias the optimization toward positive pairs and reduce discriminability. Intermediate settings (e.g., $\omega=2-3$) provide the most effective trade-off.

14. Visualization

Figure 8 shows the description of commercial LVLMs for the adversarial images generated by SADCA. It can be seen that it is capable of effectively attacking various commercial MLLMs.

Table 6. Performance of ASR (%) on open-source MLLMs across both targeted and untargeted settings on MME dataset.

Targeted	Victim Black-box Open-Source Models				
	Qwen2.5-VL-7B-Instruct	InternVL3-8B	LLaVa-1.5-7B	glm-4.1v-9b-thinking	Average
M-Attack	9.94	44.23	35.38	34.46	31.00
FOA-Attack	11.20	47.09	36.98	38.50	33.44
MPCAttack	11.88	59.81	42.29	43.39	39.34
Untargeted	Victim Black-box Open-Source Models				
	Qwen2.5-VL-7B-Instruct	InternVL3-8B	LLaVa-1.5-7B	glm-4.1v-9b-thinking	Average
M-Attack	26.20	30.92	70.18	24.68	38.00
FOA-Attack	26.20	32.69	71.52	24.68	38.77
MPCAttack	31.84	45.32	83.49	31.59	48.06

Table 7. Performance of ASR (%) on closed-source MLLMs across both targeted and untargeted settings on MME dataset.

Targeted	Victim Black-box Closed-Source Models				
	GPT-4o	GPT-5	Claude-3.5	Gemini-2.0	Average
M-Attack	53.67	27.91	4.38	25.19	27.79
FOA-Attack	55.91	30.13	6.97	31.06	31.02
MPCAttack	63.42	35.95	10.03	36.09	36.37
Untargeted	Victim Black-box Closed-Source Models				
	GPT-4o	GPT-5	Claude-3.5	Gemini-2.0	Average
M-Attack	38.34	41.10	59.64	31.91	42.75
FOA-Attack	38.50	39.91	60.13	32.17	42.68
MPCAttack	48.88	45.02	64.08	37.62	48.90

Table 8. The Average ASR (%) and AvgSim on four black-box open-source models under defense mechanisms and diverse settings.

Targeted	DiffPure		Noisy	
	ASR(↑)	AvgSim(↑)	ASR(↑)	AvgSim(↑)
M-Attack	15.05	0.1656	27.75	0.2541
FOA-Attack	17.43	0.1849	30.85	0.2831
MPCAttack	38.50	0.3330	50.85	0.4136
Untargeted	ASR(↑)		AvgSim(↓)	
	ASR(↑)	AvgSim(↓)	ASR(↑)	AvgSim(↓)
M-Attack	48.28	0.4410	59.23	0.3591
FOA-Attack	53.73	0.4036	64.35	0.3272
MPCAttack	78.13	0.2207	83.03	0.1742

Table 9. Ablation study for Multi-Paradigm.

Targeted	Victim Black-box Open-Source Models							
	Qwen2.5-VL-7B		InternVL3-8B		LLaVa-1.5-7B		GLM-4.1V-9B-Thinking	
Methods	ASR(↑)	AvgSim(↑)	ASR(↑)	AvgSim(↑)	ASR(↑)	AvgSim(↑)	ASR(↑)	AvgSim(↑)
M-Attack	17.3	0.1919	68.1	0.5361	59.9	0.4954	31.0	0.3118
M-Attack+Multi-Paradigm	24.2	0.2508	79.7	0.6117	69.6	0.5476	33.0	0.3088
FOA-Attack	20.0	0.2222	72.3	0.5700	63.8	0.5162	38.3	0.3522
FOA-Attack+Multi-Paradigm	32.7	0.3061	84.3	0.6454	72.9	0.5707	42.4	0.3760
MPCAttack	32.5	0.3191	88.7	0.6678	73.9	0.5905	58.2	0.4756
Untargeted	Victim Black-box Open-Source Models							
	Qwen2.5-VL-7B		InternVL3-8B		LLaVa-1.5-7B		GLM-4.1V-9B-Thinking	
Methods	ASR(↑)	AvgSim(↓)	ASR(↑)	AvgSim(↓)	ASR(↑)	AvgSim(↓)	ASR(↑)	AvgSim(↓)
M-Attack	54.3	0.3982	90.8	0.1417	94.9	0.0819	61.2	0.3696
M-Attack+Multi-Paradigm	67.9	0.3179	96.3	0.0888	97.9	0.0527	59.2	0.3730
FOA-Attack	61.8	0.3589	93.0	0.1204	96.3	0.0659	68.1	0.3227
FOA-Attack+Multi-Paradigm	72.3	0.2821	97.0	0.0790	98.2	0.0448	69.8	0.2989
MPCAttack	84.9	0.1919	99.1	0.0341	99.3	0.0186	85.1	0.1825

Table 10. Parameter experiments of τ and ω .

Targeted	Victim Black-box Open-Source Models							
	Qwen2.5-VL-7B-Instruct		InternVL3-8B		LLaVa-1.5-7B		GLM-4.1V-9B-Thinking	
Methods	ASR(\uparrow)	AvgSim(\uparrow)	ASR(\uparrow)	AvgSim(\uparrow)	ASR(\uparrow)	AvgSim(\uparrow)	ASR(\uparrow)	AvgSim(\uparrow)
$\tau=0.05, \omega=2$	6.6	0.1306	38.1	0.3895	37.1	0.3541	21.3	0.2511
$\tau=0.1, \omega=2$	31.2	0.3081	89.7	0.6712	75.1	0.5959	60.1	0.4842
$\tau=0.2, \omega=2$	31.7	0.3051	91.3	0.6929	76.5	0.6016	62.9	0.4910
$\tau=0.3, \omega=2$	32.3	0.3140	90.9	0.6856	77.6	0.6079	59.8	0.4934
$\tau=0.4, \omega=2$	32.1	0.3054	90.6	0.6860	77.3	0.6072	61.5	0.4917
$\tau=0.5, \omega=2$	33.2	0.3137	90.5	0.6847	76.7	0.6032	61.2	0.4893
$\tau=0.2, \omega=0.5$	11.9	0.1620	36.9	0.3748	31.7	0.3256	22.7	0.2546
$\tau=0.2, \omega=1$	26.3	0.2726	82.5	0.6173	68.3	0.5357	53.8	0.4430
$\tau=0.2, \omega=3$	34.1	0.3100	90.7	0.6855	76.4	0.6058	59.0	0.4858
$\tau=0.2, \omega=4$	30.1	0.2946	89.8	0.6870	76.6	0.6057	59.2	0.4771
$\tau=0.2, \omega=5$	14.8	0.1878	77.8	0.5854	62.5	0.5094	41.2	0.3648
Untargeted	Victim Black-box Open-Source Models							
	Qwen2.5-VL-7B-Instruct		InternVL3-8B		LLaVa-1.5-7B		GLM-4.1V-9B-Thinking	
Methods	ASR(\uparrow)	AvgSim(\downarrow)	ASR(\uparrow)	AvgSim(\downarrow)	ASR(\uparrow)	AvgSim(\downarrow)	ASR(\uparrow)	AvgSim(\downarrow)
$\tau=0.05, \omega=2$	75.8	0.2525	98.7	0.0440	99.4	0.0282	78.0	0.2464
$\tau=0.1, \omega=2$	86.6	0.1775	99.3	0.0322	99.5	0.0195	86.3	0.1665
$\tau=0.2, \omega=2$	83.6	0.1836	99.1	0.0332	99.3	0.0209	87.7	0.1620
$\tau=0.3, \omega=2$	85.5	0.1847	99.6	0.0306	99.5	0.0188	86.7	0.1621
$\tau=0.4, \omega=2$	84.6	0.1886	99.4	0.0304	99.6	0.0186	86.5	0.1688
$\tau=0.5, \omega=2$	86.4	0.1812	99.6	0.0316	99.4	0.0198	88.6	0.1610
$\tau=0.2, \omega=0.5$	90.3	0.1447	99.8	0.0148	99.6	0.0111	87.8	0.1632
$\tau=0.2, \omega=1$	86.4	0.1623	99.8	0.0221	99.8	0.0147	90.1	0.1486
$\tau=0.2, \omega=3$	83.7	0.2034	99.1	0.0386	99.5	0.0207	85.7	0.1799
$\tau=0.2, \omega=4$	80.8	0.2207	99.2	0.0407	99.1	0.0243	83.4	0.1981
$\tau=0.2, \omega=5$	69.3	0.2974	98.9	0.0549	99.3	0.0295	74.9	0.2625

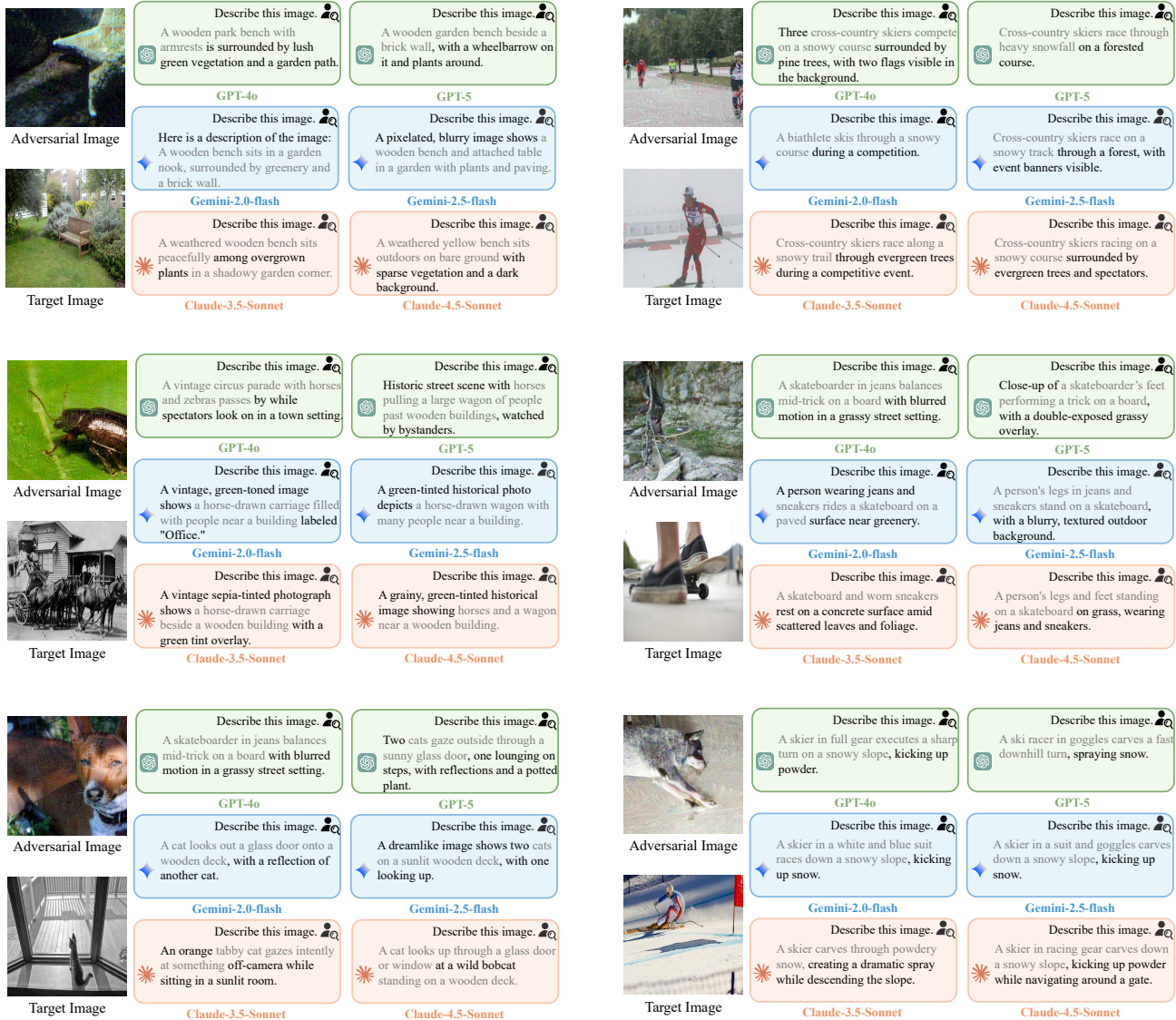


Figure 8. Visualization of adversarial images in attacking commercial MLLMs.